Design of an efficient algorithm for fuel-optimal look-ahead control

Erik Hellström, Jan Åslund and Lars Nielsen

Original Publication:

Erik Hellström, Jan Åslund and Lars Nielsen, Design of an efficient algorithm for fuel-optimal look-ahead control, 2010, Control Engineering Practice.
http://dx.doi.org/10.1016/j.conengprac.2009.12.008

Design of an efficient algorithm for fuel-optimal look-ahead control

Erik Hellström, Jan Åslund, and Lars Nielsen
Linköping University, Linköping, Sweden

Abstract

A fuel-optimal control algorithm is developed for a heavy diesel truck that utilizes information about the road topography ahead of the vehicle when the route is known. A prediction model is formulated where special attention is given to properly include gear shifting. The aim is an algorithm with sufficiently low computational complexity. To this end, a dynamic programming algorithm is tailored, and complexity and numerical errors are analyzed. It is shown that it is beneficial to formulate the problem in terms of kinetic energy in order to avoid oscillating solutions and to reduce linear interpolation errors. A residual cost is derived from engine and driveline characteristics. The result is an on-board controller for an optimal velocity profile and gear selection.

1 Introduction

A drive mission for a heavy truck is studied where there is road data on-board and the road slope ahead of the vehicle is known. The mission is given by a route and a desired maximum trip time, and the objective is to minimize the energy required for a given mission. Experimental results (Hellström et al., 2009) have confirmed that the fuel economy is improved with this approach, and the current main challenge is the efficient solution of the optimal control problem.

Related works for energy optimal control are found in other application areas such as trains (Howlett et al., 1994; Franke et al., 2002; Liu and Golovitcher, 2003) and hybrid electric vehicles (Sciarretta et al., 2004; Back, 2006; Guzzella and Sciarretta, 2007). Fuel-optimal solutions for vehicles on basic topographic road profiles are obtained in Schwarzkopf and Leipnik (1977); Monastyrsky and Golownykh (1993); Chang and Morlok (2005); Fröberg et al. (2006); Ivarsson et al. (2009). Predictive cruise control is investigated through computer simulations in, e.g., Lattemann et al. (2004); Terwen et al. (2004); Huang et al. (2008); Passenberg et al. (2009). In Hellström et al. (2006) a predictive cruise controller is developed where discrete dynamic programming is used to numerically solve the optimal control problem. In Hellström et al. (2009) the approach was evaluated in real experiments where the road slope was estimated by the method in Sahlholm and Johansson (2009).

The purpose of the present paper is to develop an optimization algorithm that finds the optimal control law for a finite horizon. The algorithm should be sufficiently robust and simple in order to be used on-board a vehicle in a real environment, and with reduced computational effort compared to previous works. Some distinguishing features of the optimization problem are that it contains both real and integer variables, and that the dimension of the state space is low. Here, an algorithm based on dynamic programming (DP) (Bellman, 1957) that finds the optimal control law is developed. Applying DP for high order systems is usually unfeasible due to exponential increase of the complexity due to the discretization of the continuous variables (Bellman, 1961), but this is not an issue in this application, since the dimension is low. Alternatively, an open-loop optimal control problem can be solved on line repeatedly for the current state to achieve feedback. These approaches are generally indirect methods based on the maximum principle (Bryson and Ho, 1975) or direct methods based on transcription (Betts, 2001). For mixed-integer nonlinear optimization, a complex combinatorial problem typically arises with the open-loop approaches due to the integer variables (Floudas, 1995). For DP, however, the computational complexity is linear in the horizon length which is beneficial for this application since a rather long horizon is needed (Hellström, 2007; Hellström et al., 2009).

Starting out the paper, a generic analysis is presented, and the model structure is defined. The first idea to reduce complexity is to obtain a better estimate of the residual cost at the end of the horizon, so that a shorter horizon can be used. By reducing the search space at each position the computational complexity can be improved further. Based on an energy formulation of the dynamics and an analysis of the discretization errors, it is shown that a coarser grid for numerical interpolation together with a simple integration method can be used.

2 Objective

The objective is to minimize the fuel M required for a drive mission with a given maximum trip time T_0:

$$\begin{aligned} &\text{minimize } M \\ &\text{s.t.} \quad T \leq T_0 \end{aligned} \tag{P1}$$

It is possible to control accelerator, brake and gear shift. Constraints on, e.g., velocity and control signals may also be included in the problem statement.

Since the road slope is a function of position, it is natural to formulate the vehicle model using spatial coordinates. A simple model may have gear and, e.g., velocity as states. Studying (P1), the time spent so far also has to be considered. A straightforward way to handle this is to include the trip time as an additional state.

The model is discretized and dynamic programming (DP) is used for the optimization. The complexity in DP grows exponentially with the number of states which is known as the *Curse of dimensionality* (Bellman, 1961). The first step to avoid this is to consider an alternative formulation of the optimization problem (P1). This is obtained by adjoining the trip time to the criterion in (P1) yielding

$$\text{minimize } M + \beta T \tag{P2}$$

where β is a scalar representing the trade-off between fuel consumption and trip time. This is the approach taken in Monastyrsky and Golownykh (1993). With this formulation, it is no longer necessary to introduce time as an additional state. Instead, there is an additional issue tuning the parameter β.

For a given β, the solution for (P2) gives a trip time $T(\beta)$. This function is not known explicitly in general. The optimal policy for (P2), for a given β, is also the optimal policy for (P1) with $T_0 = T(\beta)$, since the minimum is attained in the limit for a realistic setup. Thus, problem (P1) can be solved through (P2) if β is found such that $T(\beta) = T_0$. The function $T(\beta)$ is monotonically decreasing and β may be found by, e.g., using simple shooting methods.

The conditions may change during a drive mission due to disturbances, e.g., delays due to traffic, or changed parameters such as the vehicle mass. New optimal solutions must then be computed during the drive mission. An efficient approach is to only consider a truncated horizon in each optimization. This method gives an approximate solution to problem (P1) where the accuracy depends on the length of the truncated horizon.

3 A generic analysis

Consider the motion of a vehicle in one dimension, see Figure 1. The propelling force is F_p. The drag force is dependent on the position s and the velocity v, and is given by the function $F_d(s, v)$. It is assumed that this function is monotonically increasing for

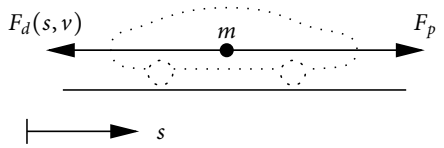

Figure 1: A vehicle moving in one dimension.

positive v, that is

$$\frac{\partial F_d}{\partial v} \geq 0, v > 0 \tag{1}$$

which should hold for any physically plausible resistance function. The problem of finding the velocity trajectory, that minimizes the work required to move the vehicle from one point $s = 0$ to another point $s = S$, is now studied.

Newton's second law of motion in spatial coordinates is

$$mv\frac{dv}{ds} = F_p - F_d(s,v) \tag{2}$$

The propulsive work equals

$$\begin{aligned} W &= \int_0^S F_p \, ds = \int_0^S \left(mv\frac{dv}{ds} + F_d(s,v) \right) ds \\ &= \frac{m}{2}\left(v(S)^2 - v(0)^2 \right) + \int_0^S F_d(s,v) \, ds \end{aligned} \tag{3}$$

that is, the sum of the difference in kinetic energy and the work due to the resisting force along the path.

The problem objective is now stated as

$$\min_{v(s)} \int_0^S \left(mv(s)\frac{dv(s)}{ds} + F_d(s, v(s)) \right) ds \tag{4}$$

with the time constraint expressed as

$$\int_0^S \frac{ds}{v(s)} \leq T_0 \tag{5}$$

where T_0 denotes the desired maximum time.

If the inequality in (5) is replaced by an equality, the resulting problem is an isoperimetric problem. For a functional $\int F(s, v, v') \, ds$ and a constraint $\int G(s, v, v') \, ds = C$ the Euler–Lagrange equation in the calculus of variations is

$$\frac{\partial F^*}{\partial v} - \frac{d}{ds}\frac{\partial F^*}{\partial v'} = 0, \quad F^* = F + \lambda G \tag{6}$$

where λ is a constant (Gelfand and Fomin, 1963). Only smooth solutions will be considered, so it is assumed that the studied functional has continuous first and second order

derivatives in the considered interval for arbitrary v and v'. In the present problem (4) and (5), the functional

$$\int_0^S \left(mv\frac{dv}{ds} + F_d + \frac{\lambda}{v} \right) ds \tag{7}$$

is formed where λ is a constant. Then, according to the Euler equation

$$m\frac{dv}{ds} + \frac{\partial F_d}{\partial v} - \frac{d}{ds}(mv) + \lambda\left(-\frac{1}{v^2}\right) = 0 \tag{8}$$

should be satisfied which yields that

$$v^2\frac{\partial}{\partial v}F_d(s,v) = \lambda \tag{9}$$

is a necessary condition for the objective to have an extremum for a function $v(s)$. Due to the assumption (1), the multiplier λ will be positive. Relaxing the equality constraint to the inequality (5) does not alter the solution. Every $v(s)$ that becomes admissible when the equality constraint is replaced with an inequality will have a higher value of the objective (4) due to (1).

In order to proceed, assume that the resistance function is a sum of two functions with explicit dependency on s and v respectively, that is

$$F_d(s,v) = f_1(s) + f_2(v) \tag{10}$$

The condition (9) then becomes

$$v^2\frac{\partial}{\partial v}f_2(v) = \lambda. \tag{11}$$

For a given λ, the solution to (11) is constant velocity. To minimize the work for moving the body from one point to another point, the extremum is thus a constant speed level adjusted to match the desired trip time.

3.1 Observations

For the general longitudinal vehicle model, depicted in Figure 1, constant speed is the solution to the problem of minimizing the needed work to move from one point to another with a trip time constraint. The assumptions are that the velocity and acceleration are smooth and that (1), (2), and (10) holds. However, due to the large mass of a heavy truck, it is not possible to keep a desired cruising speed, and the thereby unavoidable gear shifts have a noteworthy influence on vehicle motion. Therefore, the mass is the most important parameter in the current context and gear selection should be considered.

4 Truck model

The physical models are now presented. First, in the general form that is treated by the algorithm. Explicit models in this form are then given in Section 4.1–4.4. In the last section, an approximation of the explicit models is discussed.

Table 1: Longitudinal forces.

Force	Explanation	Expression
$F_a(v)$	Air drag	$\frac{1}{2}c_w A_a \rho_a v^2$
$F_r(s)$	Rolling resistance	$mg_0 c_r \cos\alpha(s)$
$F_g(s)$	Gravitational force	$mg_0 \sin\alpha(s)$

With constant gear number, i.e., between gear shifts, the vehicle acceleration is given by

$$\frac{dv}{ds} = f(s, v, g, u) \tag{12}$$

where s is the position, v is the velocity, u is the control signals and g is the gear number. The fuel mass flow is given by

$$\dot{m} = h(v, g, u) \tag{13}$$

and the consumption is obtained by integrating the flow.

A gear shift, from g_1 to g_2 with initial speed v_1, is modeled by the required time for the shift,

$$\Delta t = \xi(s, v_1, g_1, g_2) \tag{14}$$

the required distance,

$$\Delta s = \varphi(s, v_1, g_1, g_2) \tag{15}$$

the change in velocity,

$$\Delta v = v_2 - v_1 = \chi(s, v_1, g_1, g_2) \tag{16}$$

and the consumed fuel

$$\Delta m = \psi(s, v_1, g_1, g_2) \tag{17}$$

The model structure given by (12)–(17) is used in the optimization. Now, explicit models are given.

4.1 Longitudinal model

A model for the longitudinal dynamics of a truck is formulated (Kiencke and Nielsen, 2005). The vehicle is considered as a point mass moving in one dimension, see Figure 1.

The engine torque T_e is given by

$$T_e = f_e(\omega_e, u_f) \tag{18}$$

where ω_e is the engine speed and u_f is the fueling control signal. The function f_e is a look-up table originating from measurements. The clutch, propeller shafts and drive shafts are stiff. The resulting conversion ratio of the transmission and final drive $i(g)$ and their efficiency $\eta(g)$ are functions of the engaged gear number, denoted by g. The models of the resisting forces are explained in Table 1.

The relation

$$v = r_w \omega_w = \frac{r_w}{i} \omega_e \tag{19}$$

Table 2: Truck model parameters.

I_l	Lumped inertia	c_w	Air drag coefficient
I_e	Engine inertia	A_a	Cross section area
m	Vehicle mass	ρ_a	Air density
r_w	Wheel radius	c_r	Rolling res. coeff.
g_0	Gravity constant		

is assumed to hold where r_w is the effective wheel radius. Introduce the mass factor

$$c = 1 + \frac{I_l + \eta i^2 I_e}{m r_w^2}$$

Now, when a gear is engaged the forces in (2) are

$$F_p = \frac{1}{c r_w} \left(i \eta T_e(v, g, u_\mathrm{f}) - T_b(u_\mathrm{b}) \right) \tag{20a}$$

$$F_d(s, v) = \frac{1}{c} \left(F_a(v) + F_r(s) + F_g(s) \right) \tag{20b}$$

Note that the conditions (1) and (10) hold for (20b). The model (12) is now defined by

$$mv \frac{dv}{ds} = mv f(s, v, g, u) = F_p - F_d(s, v) \tag{21}$$

The states are the velocity v and currently engaged gear g, and the controls are fueling u_f, braking u_b and gear u_g. The road slope is given by $\alpha(s)$ and the brake torque is denoted by T_b. All model parameters are explained in Table 2.

4.2 Fuel consumption

The mass flow of fuel $\dot{m}$ is determined by the fueling level u_f and the engine speed ω_e. With (19), the mass flow is

$$\dot{m} = h(v, g, u) = \frac{n_{cyl}}{2\pi n_r} \omega_e u_\mathrm{f} = \frac{n_{cyl}}{2\pi n_r} \frac{i}{r_w} v u_\mathrm{f} \tag{22}$$

where n_{cyl} is the number of cylinders and n_r is the number of engine revolutions per cycle.

4.3 Neutral gear modeling

When neutral gear is engaged $g = 0$, the engine transmits zero torque to the driveline. The ratio i and efficiency η are undefined since the engine is decoupled from the rest of the powertrain. The approach taken here is to define the ratio and efficiency of neutral gear to be zero. Then, Equation (21) with $i(0) = \eta(0) = 0$ describes the vehicle motion.

4.4 Gear shift modeling

The transmission is of the automated manual type and gear shifts are carried out by engine control. In order to engage neutral gear without using the clutch, the transmission should first be controlled to a state where no torque is transmitted. The engine torque should then be controlled to a state where the input and output revolution speeds of the transmission are synchronized when the new gear is engaged. In the case of a truck with a large vehicle mass, the influence of the time with no engine propulsion becomes significant. Therefore, a model is formulated that is simple but also includes this effect.

Consider a gear shift from g_1 to g_2 with vehicle initial speed v_1. The currently engaged gear $g(t)$ is then described by

$$g(t) = \begin{cases} g_1 & t < 0 \\ 0 & 0 \le t \le \tau \\ g_2 & t > \tau \end{cases} \tag{23}$$

where τ is chosen to be constant, and hence the function in (14) is

$$\Delta t = \xi(s, v_1, g_1, g_2) = \tau \tag{24}$$

The vehicle motion $v(t)$ is given by solving the initial value problem given by (21) with $g = 0$ on $t \in [0, \tau]$ where $v(0) = v_1$. The required distance (15) is then given by integrating $v(t)$ over the interval,

$$\Delta s = \varphi(s, v_1, g_1, g_2) = \int_0^\tau v(t)\, dt \tag{25}$$

and the function in (16) becomes

$$\Delta v = \chi(s, v_1, g_1, g_2) = v(\tau) - v_1 \tag{26}$$

Fueling is required to synchronize the engine speed with the corresponding speed of the next gear in case of a down-shift. When neutral gear is engaged,

$$I_e \dot{\omega}_e = T_e = f_e(\omega_e, u_\mathrm{f}) \tag{27}$$

holds. Since the velocity trajectory is known through (21), the initial value ω_0 and desired final value ω_1 of the engine speed are also known through (19). Synchronizing the engine speed is thus equivalent to changing the rotational energy for the engine inertia by $I_e(\omega_1^2 - \omega_0^2)/2$. The consumed fuel is then estimated by

$$\Delta m = \psi(s, v_1, g_1, g_2) = \gamma \frac{1}{2} I_e(\omega_1^2 - \omega_0^2) \tag{28}$$

where γ (g/J) is introduced in Section 6.

4.5 Energy formulation

The model can be reformulated in terms of energy. Introduce the kinetic energy

$$e = \frac{1}{2} mv^2 \tag{29}$$

With the relation

$$\frac{dv}{dt} = v\frac{dv}{ds} = \frac{1}{2}\frac{d}{ds}v^2$$

a model with the structure (2) then becomes

$$\frac{de}{ds} = F_p - F_d\left(s, \sqrt{2e/m}\right) \tag{30}$$

4.6 Basic model

A basic model is derived as an approximation of the explicit model (21) for the purpose of analytical calculations later on. The speed dependence in engine torque is neglected, i.e., $T_e(v, g, u_f) \approx T(u_f)$. The approximation is typically reasonable, see Section 6 and Figure 4. For a given gear and without braking the propelling force in (2) becomes

$$F_p = \frac{i\eta}{cr_w} T(u_f) \tag{31}$$

The drag force $F_d(s, v)$ in (2) is still given by (20b).

5 Look-ahead control

Look-ahead control is a control scheme with knowledge about some of the future disturbances, here focusing on the road topography ahead of the vehicle. An optimization is performed with respect to a criterion that involves predicted future behavior of the system, and this is accomplished through DP (Bellman, 1961; Bertsekas, 1995).

5.1 Discretization

The models (12)–(17) are discretized in order to obtain a discrete process model

$$x_{k+1} = F_k(x_k, u_k)$$

where x_k, u_k denotes the state and control vectors.

Dividing the distance of the entire drive mission into M steps, the problem faced is to find

$$J_0^*(x_0) = \min_{u_0,\ldots,u_{M-1}} \zeta_M(x_M) + \sum_{k=0}^{M-1} \zeta_k(x_k, u_k) \tag{32}$$

where ζ_k and ζ_M defines the step cost and the terminal cost, respectively. The step cost is defined in Equations (38)–(40) and (44)–(45), see Section 5.4–5.5. The terminal cost is handled by introducing a residual cost in the following section.

5.2 Receding horizon

The approach taken here is to construct a look-ahead horizon by truncating the entire drive mission horizon of M steps to $N < M$ steps and approximating the cost-to-go at stage N. The shorter horizon is used in the on-line optimization. Rewrite problem (32) as

$$\begin{aligned} J_0^*(x_0) &= \min_{u_0,\ldots,u_{M-1}} \left\{ \zeta_M(x_M) + \sum_{k=0}^{M-1} \zeta_k(x_k, u_k) \right\} \\ &= \min_{u_0,\ldots,u_{N-1}} \left\{ \sum_{k=0}^{N-1} \zeta_k(x_k, u_k) + \min_{u_N,\ldots,u_{M-1}} \left\{ \zeta_M(x_M) + \sum_{k=N}^{M-1} \zeta_k(x_k, u_k) \right\} \right\} \end{aligned}$$

and define the residual cost

$$J_N^*(x_N) = \min_{u_N,\ldots,u_{M-1}} \zeta_M(x_M) + \sum_{k=N}^{M-1} \zeta_k(x_k, u_k) \tag{33}$$

as the cost-to-go function at stage N. Replace this function with an approximation $\tilde{J}_N^*(x_N)$ that should be available at a low computational effort. The problem is now only defined over the look-ahead horizon and

$$\min_{u_0,\cdots,u_{N-1}} \tilde{J}_N^*(x_N) + \sum_{k=0}^{N-1} \zeta_k(x_k, u_k) \tag{34}$$

is to be solved.

5.3 Dynamic programming algorithm

Denote by U_k the set of allowed controls and by S_k the set of allowed states at stage k. The DP solution to the look-ahead problem (34) is as follows.

1. For $x \in S_N$, let $J_N(x) = \tilde{J}_N^*(x)$.
2. Let $k = N - 1$.
3. For $x \in S_k$, let
$$J_k(x) = \min_{u \in U_k} \left\{ \zeta_k(x, u) + J_{k+1}(F_k(x, u)) \right\} \tag{35}$$
4. Repeat (3) for $k = N - 2, N - 3, \ldots, 0$.
5. The solution is made up of the policy with the optimal cost $J_0^*(x_0) = J_0(x_0)$.

The basic principle in the algorithm above is that if the cost-to-go $J_l(x)$ is known for $l \geq n$, then the cost-to-go $J_l(x)$ for $l = n - 1$ can be computed as a function of $J_l(x),\ l \geq n$.

Now consider the model in Section 4. Introduce the discretized position $s_n = nh_s$ and velocity $v_m = mh_v$, where h_s, h_v are the respective step lengths. The gear number g is assumed to be discrete.

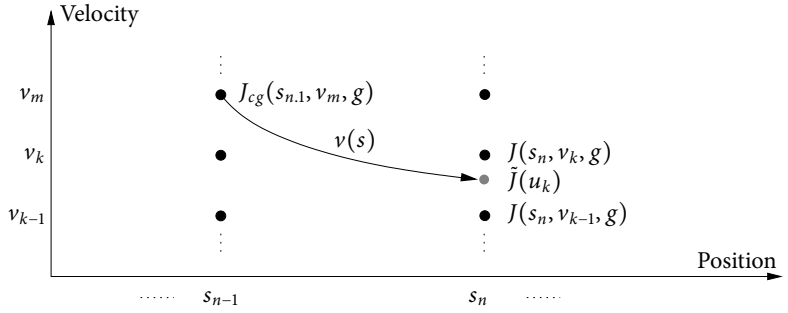

Figure 2: Cost-to-go for constant gear.

For a given velocity v_m and gear number g, the cost-to-go is $J_l(x) = J(s_l, v_m, g)$. The cost-to-go is first computed under the assumption that there is no gear shift and the result is denoted by $J_{cg}(s_{n-1}, v_m, g)$. After that, gear shifts are considered and the cost-to-go with a gear shift, $J_{gs}(s_{n-1}, v_m, g)$, is calculated. Finally, the cost-to-go is given by

$$J(s_{n-1}, v_m, g) = \min\left\{J_{cg}(s_{n-1}, v_m, g), J_{gs}(s_{n-1}, v_m, g)\right\} \tag{36}$$

The expressions for the cost-to-go for the respective case are derived in the following.

5.4 Cost-to-go for constant gear

Consider the case of constant gear g. For every discretized value u_k of the control, the solution to

$$\begin{aligned} \frac{dv}{ds} &= f(s, v(s), g, u_k), \quad s \in (s_{n-1}, s_n) \\ v(s_{n-1}) &= v_m \end{aligned} \tag{37}$$

gives a trajectory $v(s)$. The cost-to-go at the position s_n and velocity $v(s_n)$ is given by linear interpolation of $J(s_n, v_{k-1}, g)$ and $J(s_n, v_k, g)$ where $v_{k-1} \le v(s_n) \le v_k$, see Figure 2. The interpolated value is denoted by $\tilde{J}(u_k)$. The consumed fuel is

$$\Delta M = \int_{s_{n-1}}^{s_n} h(v(s), g, u_k) \frac{ds}{v(s)} \tag{38}$$

and the time spent is

$$\Delta T = \int_{s_{n-1}}^{s_n} \frac{ds}{v(s)} \tag{39}$$

where $v(s)$ is the solution of (37). The step cost is

$$\zeta_{cg}(u_k) = \Delta M + \beta \Delta T \tag{40}$$

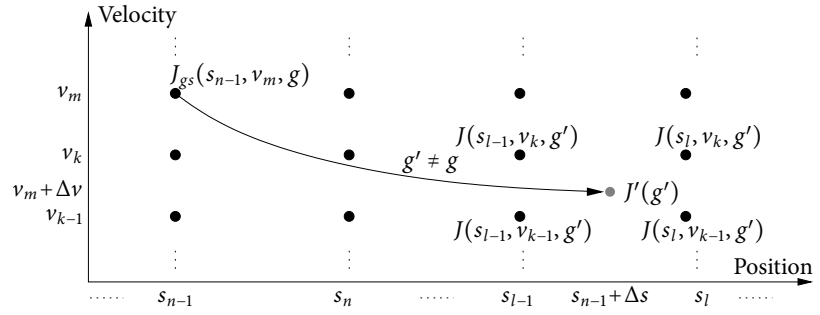

Figure 3: Cost-to-go for a gear shift.

where the terms are given by (38)–(39). The cost-to-go at position s_{n-1} and velocity v_m is obtained by finding the control signal u_k that minimizes the sum of the cost-to-go at position s_n and the step cost:

$$J_{cg}(s_{n-1}, v_m, g) = \min_{u_k} \left\{ \zeta_{cg}(u_k) + \tilde{J}(u_k) \right\} \tag{41}$$

5.5 Cost-to-go with gear shift

Consider a gear shift from gear g to $g' \neq g$ where the shift is initiated at position s_{n-1}. The gear shift model equations (15) and (16) give

$$\Delta v = \chi(s_{n-1}, v_m, g, g') \tag{42}$$

$$\Delta s = \varphi(s_{n-1}, v_m, g, g') \tag{43}$$

The cost-to-go at position $s_{n-1} + \Delta s$ and the velocity $v_m + \Delta v$ is obtained by using bilinear interpolation of the values $J(s_{l-1}, v_{k-1}, g')$, $J(s_{l-1}, v_k, g')$, $J(, s_l, v_{k-1}, g')$, and $J(s_l, v_k, g')$. An illustration is given in Figure 3. The interpolated value is denoted by $J'(g')$. The step cost is

$$\zeta_{gs}(g') = \Delta M + \beta \Delta T \tag{44}$$

where the terms are given by (17) and (14),

$$\Delta M = \psi(s_{n-1}, v_m, g, g') \tag{45}$$

$$\Delta T = \xi(s_{n-1}, v_m, g, g') \tag{46}$$

The cost-to-go at position s_{n-1} and the velocity v_m is obtained by minimizing the sum of the cost-to-go at position $s_{n-1} + \Delta s$ and the step cost:

$$J_{gs}(s_{n-1}, v_m, g) = \min_{g' \neq g} \left\{ \zeta_{gs}(g') + J'(g') \right\} \tag{47}$$

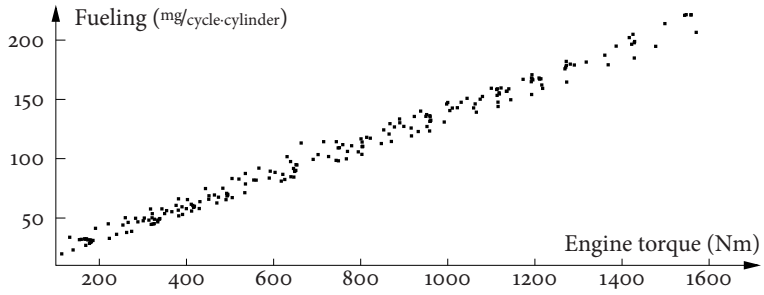

Figure 4: The relation between fueling and engine torque for a truck engine.

6 Residual cost

An approximation $\tilde{J}_N^*(x_N)$ of the residual cost (33) is now presented. The measured relation between engine torque and injected fuel mass per cycle and cylinder, for a truck engine with typical characteristics, is shown in Figure 4.

As can be seen in the figure, the function is approximately an affine function and using the method of least squares, the gradient can be calculated. By multiplying the quantities by the scaling factors $2\pi n_r \eta$ and n_{cyl}, respectively, the relation between energy (J/cycle) and fueling (g/cycle) is obtained. The gradient of the scaled function is denoted by γ, (g/J), and it indicates how much additional fuel ΔM is needed, approximately, in order to obtain a given increase of the kinetic energy Δe, i.e.

$$\Delta M \approx \gamma \Delta e$$

The basic idea in the computation of the approximate residual cost is that it is assumed that kinetic energy can be calculated to an equivalent fuel energy and conversely, at the final stage N, using the proportionality constant γ. This reflects that kinetic energy at the end of the current horizon can be used to save fuel in the future. With this assumption, the residual cost is in the form

$$\tilde{J}_N^*(x_N) = C - \gamma e \tag{48}$$

where C is an arbitrary constant that can be omitted when the optimal driving strategy is sought. In the following section, it will be shown that this approximation is accurate when no control constraint is active. It will be seen in Section 9 that this is a reasonable approximation of the residual cost in a more general case.

6.1 Cost-to-go gradient

Upper and lower bounds are derived for the difference between the cost-to-go of two neighboring states. First, introduce some short-hand notation. Denote the neighboring states at stage k by x_k^i for $i \in \{0,1\}$. The step cost is denoted by $\zeta^i = \zeta_k(x_k^i, u_k^i)$ and the cost-to-go (35) is

$$J^i = J_k(x_k^i) = \min_{u_k^i \in U_k} \left\{ \zeta^i + J_{k+1}(x_{k+1}^i) \right\}$$

where $x_{k+1}^i = F_k(x_k^i, u_k^i)$.

Now, assume that minimum is attained for u_k^0 and let $\zeta^* = \zeta^0$, then

$$J^0 = \zeta^* + J_{k+1}(x_{k+1}^0)$$

hold. Further, for any $u_k^1 \in U_k$,

$$J^1 \leq \zeta^1 + J_{k+1}(x_{k+1}^1)$$

holds. In particular, if there is an $u_k^1 \in U_k$ such that $x_{k+1}^0 = x_{k+1}^1$ then

$$\Delta J = J^1 - J^0 \leq \zeta^1 - \zeta^* \tag{49}$$

is an upper bound on the difference between the neighboring values of the cost-to-go. A lower bound can be derived analogously by assuming that the minimum is attained for u_k^1 and that there is a $u_k^0 \in U_k$ such that $x_{k+1}^0 = x_{k+1}^1$. Let $\zeta^* = \zeta^1$, then $J^1 = \zeta^* + J_{k+1}(x_{k+1}^1)$ and

$$J^0 \leq \zeta^0 + J_{k+1}(x_{k+1}^0) = \zeta^0 + J_{k+1}(x_{k+1}^1)$$

hold which can be combined into

$$\Delta J = J^1 - J^0 \geq \zeta^* - \zeta^0 \tag{50}$$

as a lower bound.

6.2 Cost-to-go gradient for basic model

The bounds in (49) and (50) are evaluated for the basic model, see Section 4.6, with the energy formulation according to (30).

Assume that constants k_1, k_2 are chosen such that the relation between fueling u and torque T fulfills

$$k_1 \leq \frac{du}{dT} \leq k_2 \tag{51}$$

Consider the upper bound (49), the difference between the step costs is given by (40) and (22),

$$\zeta^1 - \zeta^* = h_s \left[\frac{n_{cyl}}{2\pi n_r} \frac{i}{r_w} \Delta u + \beta \left(\frac{1}{\nu_k^1} - \frac{1}{\nu_k^0} \right) \right]$$

where $\Delta u = u_k^1 - u_k^0$. Assuming that $\Delta u \leq k \Delta T$ yields

$$\zeta^1 - \zeta^* \leq h_s \left[\frac{n_{cyl}}{2\pi n_r} \frac{i}{r_w} k \Delta T_e + \beta \left(\frac{1}{\nu_k^1} - \frac{1}{\nu_k^0} \right) \right] \tag{52}$$

where $\Delta T_e = T_e(u_k^1) - T_e(u_k^0)$. Applying Euler forward to (30) and solving for ΔT_e yields

$$\Delta T_e = \frac{c r_w}{i \eta} \frac{\Delta e}{h_s} \left(-1 + h_s \frac{c_w A_a \rho_a}{cm} \right)$$

where $\Delta e = e_k^1 - e_k^0$ and the value inside the parenthesis is negative for reasonable parameter values. Note that it is assumed that there is a feasible control for the required state transition. Insertion into (52), using (51), and rewriting yields

$$\zeta^1 - \zeta^* \leq \Delta e \left[\underline{\gamma} \left(-c + h_s \frac{c_w A_a \rho_a}{m} \right) - \beta \frac{h_s}{m} \frac{2}{v^0 v^1 (v^0 + v^1)} \right] \tag{53}$$

where $\underline{\gamma} = \frac{n_{cyl}}{2\pi n_r \eta} k_1$ and $v^i = \sqrt{\frac{2e_k^i}{m}}$. Thus, for a discretization where $\underline{v} \leq v \leq \overline{v}$,

$$\frac{\Delta J}{\Delta e} \leq -\underline{\gamma} \left[c - \frac{h_s}{m} \left(c_w A_a \rho_a - \frac{\beta}{\underline{\gamma} \overline{v}^3} \right) \right] \tag{54}$$

holds.

The lower bound (50) is analogously treated. This yields

$$\frac{\Delta J}{\Delta e} \geq -\overline{\gamma} \left[c - \frac{h_s}{m} \left(c_w A_a \rho_a - \frac{\beta}{\overline{\gamma} \underline{v}^3} \right) \right] \tag{55}$$

where $\overline{\gamma} = \frac{n_{cyl}}{2\pi n_r \eta} k_2$.

For a large mass, $c \approx 1$. The other two terms in the parentheses in (54) and (55) are in the order of 10^{-3} for typical parameters. Thus, the gradient of the value function with respect to kinetic energy is approximately equal to the scaled gradient γ of the fueling with respect to engine torque.

7 Complexity analysis

In the DP algorithm, the state x_k and the control signal u_k are discretized. If there are no restrictions on the search space, the number of step costs $\zeta_k(x_k, u_k)$ that have to be computed, at each gear and position, is equal to the product of the number of grid points and the number of discrete control signals.

The number of possible control signals is reduced due to physical limitations, such as limits on available propulsive force and braking force. In Figure 5 these limitations are the dashed lines. The number of control signals can be reduced even further by taking into account that different optimal trajectories never intersect. This principle is illustrated in Figure 5. First, assume that the grid is uniform, and that the optimal control for a state in the middle of the interval is computed, as shown to the left in the figure. After that the interval is divided into two the subintervals of equal length, and the optimal control is computed for the states in the middle of these subintervals. In these two computations, the possible control signals, not taking physical limitations into account, are reduced by half in average, as indicated by the gray areas in the right figure.

The interval is then divided into four subintervals of equal length and the number of computations can once again be reduced by half in average. By continuing in the same

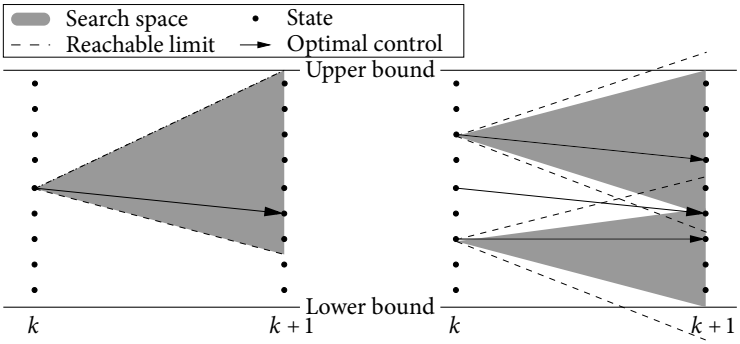

Figure 5: Reducing the possible control signals.

way and divide the state space into smaller and smaller subintervals and reducing the search space, the number of computations can be significantly reduced.

In Section 9 it will be shown that also the number of grid points can be reduced by choosing kinetic energy as a state in comparison to using velocity.

8 Discretization analysis

Performing numerical optimization of dynamical systems inevitable leads to errors such as rounding and truncation errors. It is of course desirable, but hard to guarantee, that such errors do not lead to that the numerical solution differ from the solution of the original problem.

In the following illustrating examples are presented. The observed features are then investigated by continuing the generic analysis in Section 3.

8.1 Generic analysis continued

Consider the problem of minimizing the fuel consumption, on a given gear, for a trip with a constraint on the trip time. Without other constraints, braking is intuitively never optimal and the only control left is the fueling. To study this problem the basic model is used, see Section 4.6.

Study the objective to minimize the work needed to bring the system from $s = 0,\ v(0) = v_0$ to $s = S,\ v(S) = v_0$. According to (3), the work needed is

$$W = \int_0^S F_p \, ds = \int_0^S F_d(s, v) \, ds \tag{56}$$

since the kinetic energy at the start and the end of the interval is the same. The time is constrained by

$$\int_0^S \frac{ds}{v} \leq T_0 \tag{57}$$

The engine torque is approximately an affine function in u_f, see Section 6 and Figure 4. With this approximation, the criterion (56) is equivalent to minimizing the fuel consumption. Without bounds on the control, the solution is constant speed according to Section 3. However, the fueling has natural bounds. If constant speed is feasible and the constraints are inactive then, clearly, the solution is still constant speed. Considering that the constraints possibly are active, the optimal control is analytically known to be of the type bang-singular-bang (Fröberg et al., 2006). It consists of constrained arcs with maximum or minimum fueling, and singular arcs with partial fueling such that constant speed is maintained.

In the following, the problem given by (2) and (56)–(57) is used as a test problem. Numerical solutions given by DP are presented and basic analytical calculations are performed.

For the analytical calculations three mesh points, $0 < h_s < 2h_s$ are studied. The control is assumed constant on each subinterval,

$$u_f(s) = \begin{cases} u_0 & s \in [0, h_s) \\ u_1 & s \in [h_s, 2h_s) \end{cases}$$

The objective can then be stated as

$$J = \min_{u_0, u_1} h_s \left(F_p(u_0) + F_p(u_1) \right) \tag{58}$$

using Equation (56) and where $v(0) = v_0$, $v(h) = v_1$. The maximum time T_0 is chosen as $T_0 = 2h_s/v_0$. For flat road, constant speed is feasible and the expected solution is constant speed, that is $v_1 = v_0$.

8.2 The Euler forward method

The DP solution for the test problem, using velocity as state and the Euler forward method for discretization, is shown in Figure 6. An oscillating solution appears on the flat segment where the solution is expected to be constant speed. The forward method applied to the dynamic model for simulation is stable for the step lengths used, hence such a stability analysis cannot explain the behavior. In the following, the test problem is used to investigate the oscillating behavior of the solution to the optimization problem.

The forward Euler method applied on the model (2) gives

$$\frac{v_{i+1} - v_i}{h_s} = \frac{1}{m v_i} \left(F_p(u_i) - F_d(s_i, v_i) \right) \tag{59}$$

Now, solve (59) for $F_p(u_i)$ where $i \in \{0, 1\}$ and note that, due to the terminal constraints, $v_2 = v_0$. Insertion into the objective (58) gives

$$W_{\text{ef}}(v_1) = h_s \left(F_d(s_0, v_0) + F_d(s_1, v_1) \right) - m \left(v_1 - v_0 \right)^2 \tag{60}$$

where v_1 now is the only free parameter.

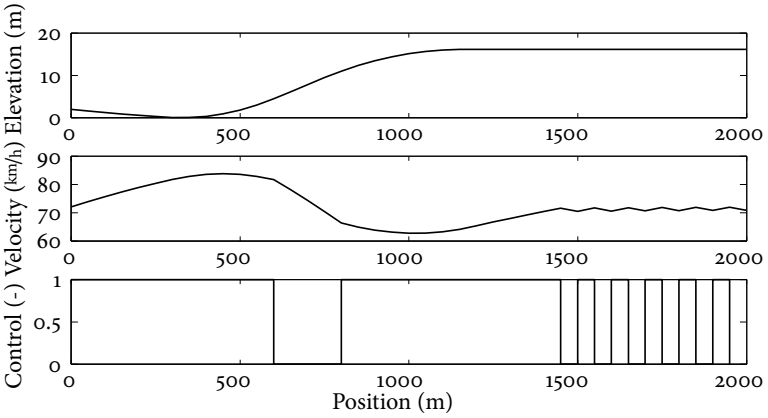

Figure 6: DP solution using velocity as state and Euler forward for discretization.

For flat road, the minimum of the objective is expected to occur for $v_1 = v_0$. Therefore,

$$W_{\text{ef}}(v_0) < W_{\text{ef}}(v_1) \quad \forall\ v_1 > v_0 \tag{61}$$

should hold. By inserting (60) into (61),

$$\frac{F_d(s_1, v_1) - F_d(s_1, v_0)}{v_1 - v_0} > m\frac{v_1 - v_0}{h_s} \tag{62}$$

is obtained. Approximating the differences with the corresponding derivatives yields

$$\frac{\partial F_d}{\partial v} > m\frac{dv}{ds} \tag{63}$$

Using (20b) and the models in Table 1 give $\partial F_d/\partial v = c_w A_a \rho_a v/c$. For typical values of a heavy truck with $m = 40 \cdot 10^3$ kg at $v = 20$ m/s, $c_w A_a \rho_a / c \approx 0.6 \cdot 10 \cdot 1.2/1 = 7.2 < 8$. Then according to (63),

$$\frac{dv}{dt} = v\frac{dv}{ds} < \frac{c_w A_a \rho_a v^2}{cm} < \frac{8 \cdot 20^2}{40 \cdot 10^3} = 0.08\ \text{m/s}^2$$

should hold but such a truck typically has a larger maximum acceleration. Therefore, the discrete optimization algorithm using this method may find these oscillating solutions.

8.3 The Euler backward method

With velocity as state and the Euler backward method for discretization, the DP solution for the test problem is shown in Figure 7. There is no longer an oscillating solution but the expected control switches between singular and constrained arcs are damped.

Applying the backward Euler method on the model (2) gives

$$\frac{v_{i+1} - v_i}{h_s} = \frac{1}{mv_{i+1}}\left(F_p(u_i) - F_d(s_{i+1}, v_{i+1})\right) \tag{64}$$

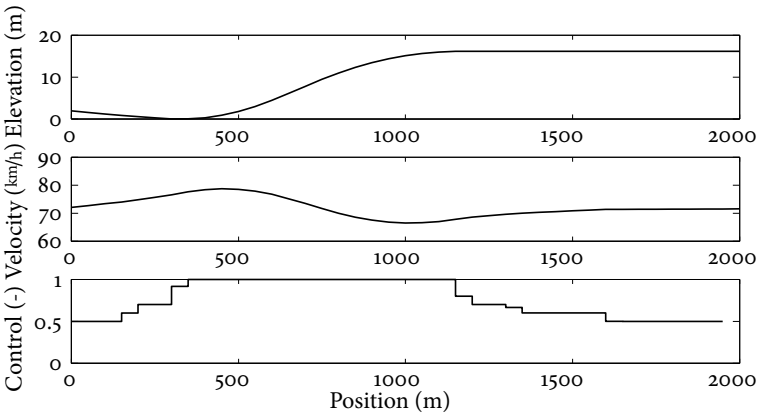

Figure 7: DP solution using velocity as state and Euler backward for discretization.

Proceed as for the Euler forward method earlier. Solve for $F_p(u_i)$ from (64) where $i \in \{0, 1\}$ and use that $v_2 = v_0$. Insertion into the objective (58) gives

$$W_{\text{eb}}(v_1) = h_s \left(F_d(s_1, v_1) + F_d(s_2, v_0) \right) + m \left(v_1 - v_0 \right)^2 \tag{65}$$

When using this method, it is seen that there is no $v_1 > v_0$ such that the objective (65) becomes lower than when $v_1 = v_0$. Thus, the method guarantees that the solution for flat road, i.e., constant speed, to the test problem is preserved. However, changes in velocity $v_1 \neq v_0$ are always penalized with the last term in (65). This is consistent with the results in Figure 7 where the expected control switches are smoothed out.

8.4 Energy formulation

With the energy formulation in (30), kinetic energy e is used as state variable instead of the velocity v. The DP solutions for the test problem, with this reformulation and the same number of grid points as before, for both Euler methods are shown in Figure 8. The bang-singular-bang characteristics now appear clearly and there are only small differences between the two Euler methods.

Performing similar calculations as previously, the objective value (58) becomes

$$W_{\text{ef}}(v_1) = h_s \left(F_d(s_0, v_0) + F_d(s_1, v_1) \right)$$
$$W_{\text{eb}}(v_1) = h_s \left(F_d(s_1, v_1) + F_d(s_2, v_0) \right)$$

Due to (1), $F_d(s, v_1) > F_d(s, v_0)$ if $v_1 > v_0$ and thus, the expected solution $v_1 = v_0$ for flat road is obtained. The objective values only consist of the resisting force evaluated in different points and there is no extra term as in (60) and (65). In conclusion, with the energy formulation, the simple Euler forward method can be used with adequate solution characteristics.

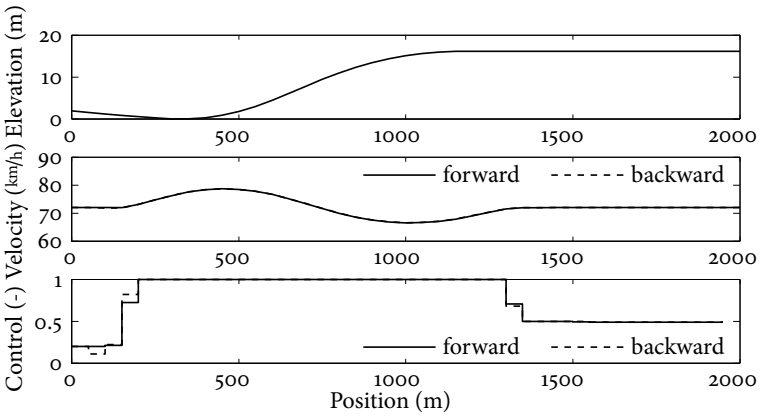

Figure 8: DP solution using kinetic energy as state and Euler methods for discretization.

9 Interpolation error

The DP algorithm is now applied on an illustrating example. The explicit truck model (21) and the energy formulation is used. The model thus has the structure (30) with forces given by (20). The road segment comes from measurements on a Swedish highway, see Figure 9.

Figure 10 shows the value function at 16 different positions with a distance between them of 200 m. The value function at position $s = 3000$ m is the proposed residual cost (48) and it can be seen that the shape of the cost function is approximately preserved for the other positions. Hence, the value function is dominated by a linear function with the gradient γ introduced in Section 6. As can be expected, the distance between the lines is smaller in the downhill segment compared to the uphill segment.

In the optimization algorithm it is the small deviations from the dominating straight line that are important. A consequence of this is that the linear interpolation error is significantly reduced if kinetic energy is used as state, instead of velocity, since the interpolation error of the dominating linear part is zero. This means that a coarser grid can be used and the complexity of the algorithm is reduced.

In Figure 11 the deviation from the linear function (48) is shown at four positions. It

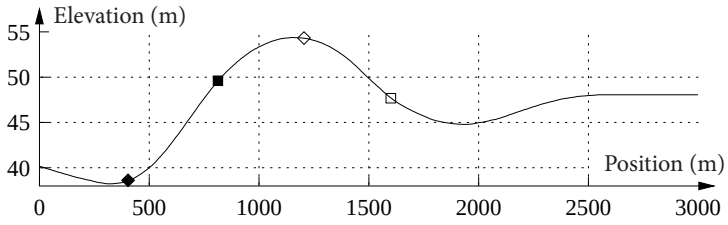

Figure 9: A road segment. The markers show the positions for the curves in Figure 11.

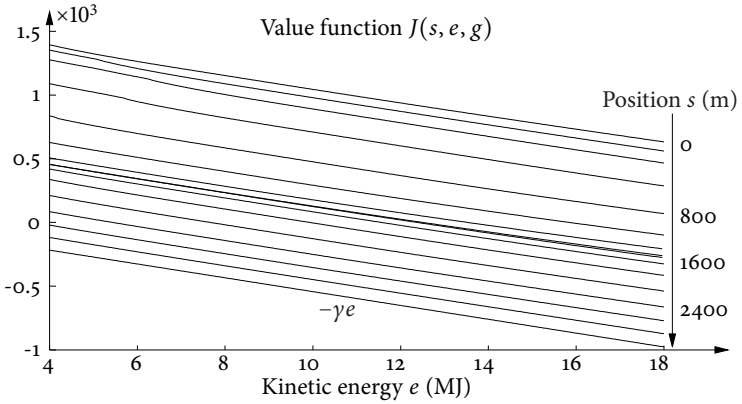

Figure 10: Value function $J(s, e, g)$ for $g = 12$.

is clearly seen that high velocities are most favorable at the beginning of the uphill slope, at 400 m, and least favorable at the top of the hill, at 1200 m. The curve for $s = 400$ m has a knee at 6 MJ, and the reason is that below this point a gear-shift is required. Low velocities are most beneficial at the top of the hill and in the downhill slope, at 1200 m and 1600 m.

10 Experimental data

A demonstrator vehicle, developed in collaboration with Scania, has been used to drive optimally according to (P2). Detailed description of the experimental situation is given in Hellström et al. (2009), and sensitivity to, e.g., mass and horizon length, is found in Hellström (2007). The trial route is a 120 km segment of a Swedish highway. In average, the fuel consumption is decreased about 3.5% without increasing the trip time and the number of gear shifts is decreased with 42% traveling back and forth, compared to the standard cruise controller. The tractor and trailer have a gross weight of about 40 tonnes. In Figure 12, measurements from a 6 km segment of the trial route are shown. The experience from the work with look-ahead is that the control is intuitive, in a qualitatively manner. The main characteristics are slowing down or gaining speed prior to significant hills. Slowing down will intuitively save fuel and reduce the need for braking. The lost time is gained by accelerating prior to uphills which also reduces the need for lower gears. However, to reduce the fuel consumption the detailed shape of the optimal solution is crucial.

The energy formulation together with the discretization and interpolation theory from Sections 8 and 9 leads to that the required resolution of the state grid is reduced compared to the straightforward velocity formulation. Note that the obtained solution is still optimal according to (P2). Furthermore, the use of simple Euler forward integration is possible since oscillations are avoided and the residual cost enables the use of a shorter horizon. Although a completely fair comparison is hard to make, all these factors reduce

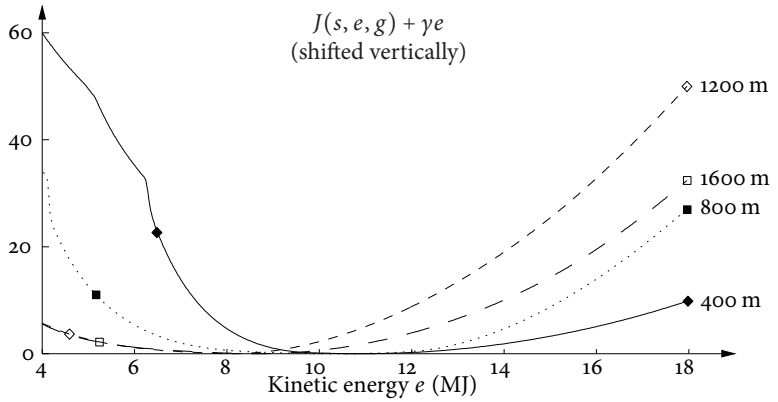

Figure 11: $J(s, e, g) + \gamma e$ for $g = 12$ and different positions s. Each curve is shifted vertically such that its minimum is zero. The markers are also shown in Figure 9.

the computation time significantly, in total approximately a factor of 10 compared to the previous implementation.

11 Conclusions

A DP algorithm for fuel-optimal control has been developed. Gear shifting is modeled by functions for the velocity change and the required time, distance, and fuel, respectively, during the shift process. A formulation that the algorithmic framework is well suited for, since it allows a proper physical model of the gear shift and can be easily handled in the algorithm by using interpolation. Furthermore, it was shown that a residual cost can be derived from engine and driveline characteristics, and the result is a linear function in energy.

The errors due to discretization and interpolation have been analyzed in order to assure a well-behaved algorithm. Depending on the choice of integration method, oscillating solutions may appear, and for that the interplay between the objective and the errors was shown to be crucial. A key point is that it is beneficial to reformulate the problem in terms of energy. It was shown that this both avoids oscillating solutions and reduces interpolation errors. A consequence is that a simple Euler forward method can be used together with a coarse grid and linear interpolation. This gives an accurate solution with low computational effort, thereby paving the way for efficient on-board fuel-optimal look-ahead control.

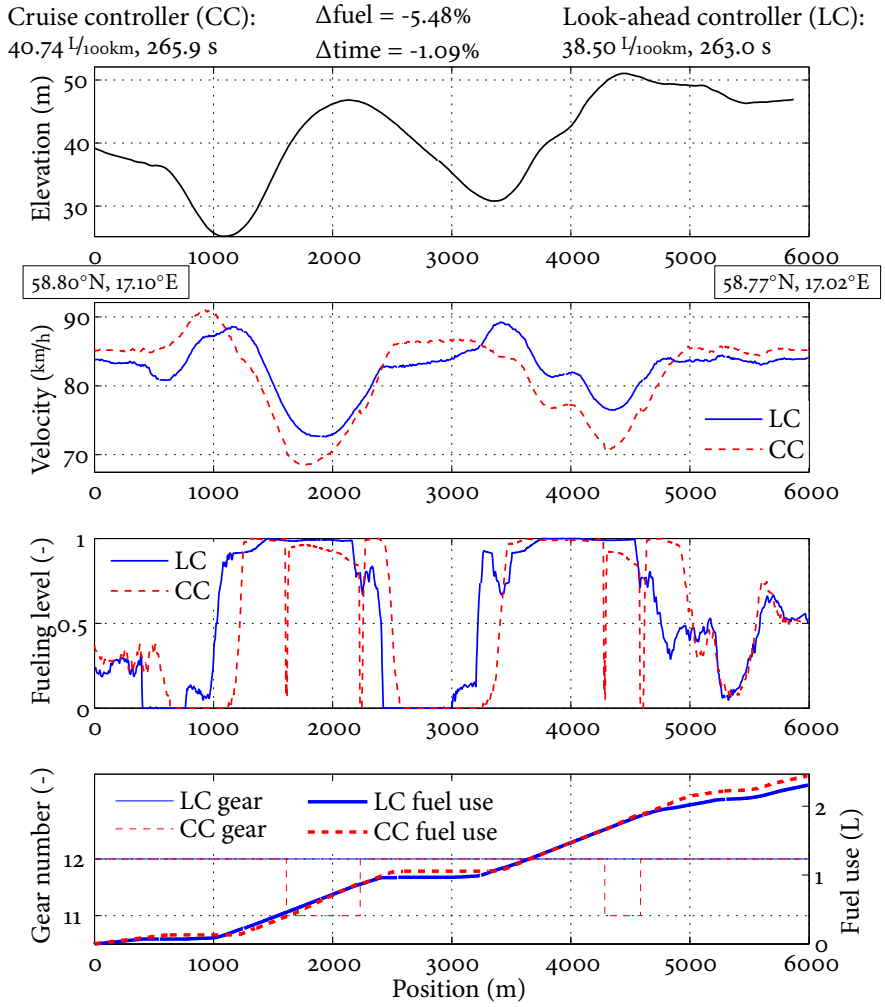

Figure 12: Measured data from one road segment. The LC travels slower prior to downhills and saves fuel. Gaining speed prior to uphills gains the lost time and also avoids gear shifts.

References

M. Back. *Prädiktive Antriebsregelung zum energieoptimalen Betrieb von Hybridfahrzeugen*. PhD thesis, Universität Karlsruhe, Karlsruhe, Germany, 2006.

R.E. Bellman. *Dynamic Programming*. Princeton University Press, Princeton, New Jersey, 1957.

R.E. Bellman. *Adaptive Control Processes: A Guided Tour*. Princeton University Press, Princeton, New Jersey, 1961.

D.P. Bertsekas. *Dynamic Programming and Optimal Control*, volume I. Athena Scientific, Belmont, Massachusetts, 1995.

J.T. Betts. *Practical methods for otpimal control using nonlinear programming*. SIAM, Philadelphia, 2001.

A.E. Bryson and Y. Ho. *Applied Optimal Control*. Taylor and Francis, 1975.

D.J. Chang and E.K. Morlok. Vehicle speed profiles to minimize work and fuel consumption. *Journal of transportation engineering*, 131(3):173–181, 2005.

C.A. Floudas. *Nonlinear and mixed-integer optimization*. Oxford Univ. Press, New York, 1995.

R. Franke, M. Meyer, and P. Terwiesch. Optimal control of the driving of trains. *Automatisierungstechnik*, 50(12):606–613, December 2002.

A. Fröberg, E. Hellström, and L. Nielsen. Explicit fuel optimal speed profiles for heavy trucks on a set of topographic road profiles. In *SAE World Congress*, number 2006-01-1071 in SAE Technical Paper Series, Detroit, MI, USA, 2006.

I.M. Gelfand and S.V. Fomin. *Calculus of variations*. Prentice-Hall, Englewood Cliffs, New Jersey, 1963.

L. Guzzella and A. Sciarretta. *Vehicle Propulsion Systems*. Springer, Berlin, 2nd edition, 2007.

E. Hellström. *Look-ahead Control of Heavy Trucks utilizing Road Topography*. Licentiate thesis LiU-TEK-LIC-2007:28, Linköping University, 2007.

E. Hellström, A. Fröberg, and L. Nielsen. A real-time fuel-optimal cruise controller for heavy trucks using road topography information. In *SAE World Congress*, number 2006-01-0008 in SAE Technical Paper Series, Detroit, MI, USA, 2006.

E. Hellström, M. Ivarsson, J. Åslund, and L. Nielsen. Look-ahead control for heavy trucks to minimize trip time and fuel consumption. *Control Engineering Practice*, 17 (2):245–254, 2009.

P.G. Howlett, I.P. Milroy, and P.J. Pudney. Energy-efficient train control. *Control Engineering Practice*, 2(2):193–200, 1994.

W. Huang, D.M. Bevly, S. Schnick, and X. Li. Using 3D road geometry to optimize heavy truck fuel efficiency. In *11th International IEEE Conference on Intelligent Transportation Systems*, pages 334–339, 2008.

M. Ivarsson, J. Åslund, and L. Nielsen. Look ahead control - consequences of a non-linear fuel map on truck fuel consumption. *Proceedings of the Institution of Mechanical Engineers, Part D, Journal of Automobile Engineering*, 223(D10):1223–1238, 2009.

U. Kiencke and L. Nielsen. *Automotive Control Systems, For Engine, Driveline, and Vehicle*. Springer-Verlag, Berlin, 2nd edition, 2005.

F. Lattemann, K. Neiss, S. Terwen, and T. Connolly. The predictive cruise control - a system to reduce fuel consumption of heavy duty trucks. In *SAE World Congress*, number 2004-01-2616 in SAE Technical Paper Series, Detroit, MI, USA, 2004.

R. Liu and I.M. Golovitcher. Energy-efficient operation of rail vehicles. *Transportation Research*, 37A:917–932, 2003.

V.V Monastyrsky and I.M. Golownykh. Rapid computations of optimal control for vehicles. *Transportation Research*, 27B(3):219–227, 1993.

B. Passenberg, P. Kock, and O. Stursberg. Combined time and fuel optimal driving of trucks based on a hybrid model. In *European Control Conference*, Budapest, Hungary, 2009.

P. Sahlholm and K.H. Johansson. Road grade estimation for look-ahead vehicle control using multiple measurement runs. *Control Engineering Practice*, 2009. doi: 10.1016/j.conengprac.2009.09.007.

A.B. Schwarzkopf and R.B. Leipnik. Control of highway vehicles for minimum fuel consumption over varying terrain. *Transportation Research*, 11(4):279–286, 1977.

A. Sciarretta, M. Back, and L. Guzzella. Optimal control of parallel hybrid electric vehicles. *IEEE Transactions on Control Systems Technology*, 12(3):352–363, 2004.

S. Terwen, M. Back, and V. Krebs. Predictive powertrain control for heavy duty trucks. In *4th IFAC Symposium on Advances in Automotive Control*, Salerno, Italy, 2004.